

Article

Accelerated System-Level Seismic Risk Assessment of Bridge Transportation Networks through Artificial Neural Network-Based Surrogate Model

Sungsik Yoon ¹, Jeongseob Kim ², Minsun Kim ², Hye-Young Tak ^{3,*} and Young-Joo Lee ^{2,*} 

¹ Department of Civil and Environmental Engineering, University of Illinois at Urbana-Champaign, Urbana, IL 61801, USA; sunsik@illinois.edu

² Department of Urban and Environmental Engineering, Ulsan National Institute of Science and Technology, 50 UNIST-gil, Eonyang-eup, Ulju-gun, Ulsan 44919, Korea; jskim14@unist.ac.kr (J.K.); minsun741@unist.ac.kr (M.K.)

³ National Territorial Planning & Regional Research Division, Korea Research Institute for Human Settlements, Sejong 30149, Korea

* Correspondence: hytak@krihs.re.kr (H.-Y.T.); ylee@unist.ac.kr (Y.-J.L.)

Received: 16 August 2020; Accepted: 15 September 2020; Published: 17 September 2020



Featured Application: Post-hazard flow capacity of the lifeline network and recovery strategy against natural disaster.

Abstract: In this study, an artificial neural network (ANN)-based surrogate model is proposed to evaluate the system-level seismic risk of bridge transportation networks efficiently. To estimate the performance of a network, total system travel time (TSTT) was introduced as a performance index, and an ANN-based surrogate model was incorporated to evaluate a high-dimensional network with probabilistic seismic hazard analysis (PSHA) efficiently. To generate training data, the damage states of bridge components were considered as the input training data, and TSTT was selected as output data. An actual bridge transportation network in South Korea was considered as the target network, and the entire network map was reconstructed based on geographic information system data to demonstrate the proposed method. For numerical analysis, the training data were generated based on epicenter location history. By using the surrogate model, the network performance was estimated for various earthquake magnitudes at the trained epicenter with significantly-reduced computational time cost. In addition, 20 historical epicenters were adopted to confirm the robustness of the epicenter. Therefore, it was concluded that the proposed ANN-based surrogate model could be used as an alternative for efficient system-level seismic risk assessment of high-dimensional bridge transportation networks.

Keywords: seismic risk assessment; bridge transportation network; surrogate model; total system travel time; artificial neural network

1. Introduction

Natural and man-made hazards can cause devastating damage to civil infrastructures, such as transportation, water, gas, and power networks. Complex lifelines have been constructed densely throughout entire cities; hence, disconnecting main components could cause not only massive direct damage (e.g., repair costs), but also indirect damage (e.g., disruption of commercial and residential activities). In particular, bridge transportation networks are extensively constructed to meet the needs of commercial, industrial, and residential activities by providing products or supplies from source to destination nodes through complex transportation systems. The frequency of recent natural disasters

necessitates seismic risk assessment for complex bridge transportation networks and a post-hazard recovery strategy. Therefore, it is essential to analyze the seismic performance of bridge transportation networks, including disconnection of major components, and assess post-hazard performance under disaster conditions [1,2].

For this purpose, numerous researchers have evaluated the performance of various lifeline networks including bridge transportation networks under seismic conditions. In previous studies, lifeline structures were analyzed through network system analysis, and the introduced analyses of system performance evaluation can be classified into connectivity- and flow-based analyses. Connectivity-based analysis identifies the connectivity between source and sink nodes by dividing the damage states of a network's components into bi-states (i.e., damaged or intact). Because such a connectivity-based method is relatively simple and easy to handle, numerous prior studies have evaluated networks based on connectivity analysis. For example, Esposito et al. [3] analyzed the seismic reliability of a gas distribution network in Italy, considering key components such as metering/pressure reducing stations of gas plants. Yoon et al. [2] performed the seismic risk analysis of a water transmission network in South Korea. In addition, Nuti et al. [4] evaluated the seismic hazards of urban-level power, water, and road networks, and Osorio et al. [5] estimated system reliability considering the interdependencies between water distribution and power networks. Rokneddin et al. [6] introduced Markov Chain Monte Carlo (MCMC) simulations to evaluate the reliability of a deteriorated highway bridge network. They also proposed a recovery priority of bridge components and recovery strategies for an entire network based on the network topology. Kang et al. [7] proposed a performance evaluation methodology for bridge transportation networks based on a non-sampling-based methodology. However, such a connectivity-based network analysis has limited accuracy in predicting network performance because it does not reflect physical conditions such as the serviceability and capacity of component facilities according to their various damage states.

To overcome this limitation, flow-based network analysis methodologies have been developed. For example, Yoon et al. [8] conducted a flow analysis of a water transmission network in South Korea by introducing a network update strategy based on pressure-driven analysis. Shi and O'Rourke [9] and Wang and O'Rourke [10] developed the GIRAFFE software to evaluate the system performance of five water network districts in the Los Angeles region, USA, against seismic conditions. Moreover, Nuti et al. [11] proposed a flow equation that considers the damage states of major components to evaluate the seismic safety of power networks in Sicily, Italy. In the case of transportation networks, Choi and Song [12] developed a multi-group non-dominated sorting genetic algorithm and conducted research to explore critical post-disaster scenarios by employing network impact measures such as network flow capacity in the Eastern Massachusetts highway network, USA, and a Jeju transportation network, South Korea. Tak et al. [13] evaluated the system-level seismic risk assessment of a bridge transportation network in South Korea based on the maximum flow capacity, which was defined as the maximum number of vehicles per unit time. Lee et al. [14] estimated the post-hazard flow capacity of a bridge transportation network in the USA considering the deterioration of the bridge. However, for bridge transportation networks, novel measures such as total system travel time (TSTT) are required because not only node-to-node capacity but also all nodes in the network can be candidates for source or destination nodes. TSTT can be introduced as a more realistic performance measure of bridge transportation networks because it is based on the travel times of all vehicles and considers the traffic and topology of the bridge transportation network. For these reasons, Sharma and Mathew [15] introduced TSTT to a multi-objective network design problem, and Chang et al. [16] adopted TSTT as a system measure to assess the physical damage and functional loss of transportation infrastructure systems. Kim et al. [17] also used TSTT to conduct a study on earthquake loss assessment and mitigation measures in the transportation network of Charleston County, South Carolina, USA. However, their research has not been applied to high-order complex network problems, but also has the disadvantage of having to calculate the TSTT directly for each scenario. Therefore, since a large

computational time cost is required to calculate the performance index of each scenario, the entire analysis time exponentially increases as the network dimension increases.

Methods for evaluating the performance of a network can be divided into sampling-based methods and non-sampling-based methods. Sampling-based methods are straightforward and easy to use; hence, various previous studies have carried out seismic risk assessments by adopting sampling-based methods such as Monte Carlo simulation (MCS) [13]. However, when an analysis necessitating MCS with a large number of samples (e.g., probabilistic seismic hazard analysis (PSHA) and network design optimization) is of interest, a sampling-based method may require a significant amount of computational time [18]. To overcome this limitation, Stern et al. [19] evaluated the seismic performance of the California water network through logistic regression and the kernel support vector classifier, and Dueñas-Osorio and Rojo [20] proposed a radial topology to measure the system reliability effectively. In addition, a non-sampling-based method, termed the matrix-based system reliability (MSR) method, has been developed in several previous studies to predict various system reliabilities [21,22]. Moreover, a recursive decomposition algorithm (RDA) was developed as another new non-sampling-based approach, and various network reliabilities have been evaluated using the RDA methodology [23–26]. However, this previous research has the disadvantage of simply performing connectivity analysis according to the bi-state of network components without taking into account the network flow analysis. Therefore, the previously proposed methods can only depict the tendency of the overall performance degradation of the network.

In addition, the existing sampling- and non-sampling-based methods have some limitations in seismic risk assessment with a robust performance measure for complex networks. Many of the existing methods have been applied only to critical urban infrastructure systems by adopting relatively simple measures of network performance such as connectivity and maximum flow capacity. Furthermore, although some researchers developed methods such as multi-scale approaches [27,28] and the branch-and-bound method [21] to deal with complex network problems, the preliminary studies have not been applied to extremely-complex network systems and have not aimed to reduce the time cost of iterative calculations for various epicenters and earthquake magnitudes. Therefore, these approaches are unsuitable for evaluating system reliability measures of complex lifeline networks with sophisticated performance measures such as TSTT.

This study proposes an accelerated methodology of system-level seismic risk assessment with a novel system performance measure. By adopting the performance measure of TSTT which considers the total travel times of the entire network system between multiple pairs of origin and destination nodes, the performance of a bridge transportation network can be measured more accurately. In addition, to reduce the computational time, an artificial neural network (ANN)-based surrogate model was employed because it is difficult to calculate the TSTT measurement directly for PSHA considering multiple epicenters and earthquake magnitudes. The surrogate model enables accelerated calculation of the novel performance index of complex networks without direct calculation of an entire framework.

To demonstrate the proposed method with an ANN-based surrogate model, an actual bridge transportation network in Pohang, South Korea, was adopted, and the network map was reconstructed based on the locations of bridges and roads. In addition, the training data for the ANN-based surrogate model were set to the epicenters and magnitudes of historical earthquake data to generate random events, and the damage states and results of TSTT simulation of the bridge were utilized as input and output data, respectively. The performance of the proposed surrogate model was verified through the correlation coefficient of the generated surrogate function. The constructed surrogate model was able to estimate the mean total travel time and relative importance of the bridge transportation network according to the various earthquake magnitudes and epicenters.

2. Proposed Method

2.1. Conventional Monte Carlo Simulation (MCS) Framework for Direct Calculation

Figure 1 shows a conventional framework for evaluating the seismic performance of bridge transportation networks based on the MCS approach. For direct calculation in a MCS framework, the network map should be reconstructed using geographic information system (GIS) data. Once an epicenter and earthquake magnitude are identified, the ground motion of the entire region of the target network can be calculated using the spatially correlated ground motion prediction equation based on the reconstructed network map. When the intensity of the ground motion is determined at the locations of bridge structures, the probabilities of bridges according to their damage states can be calculated from seismic fragility curves.

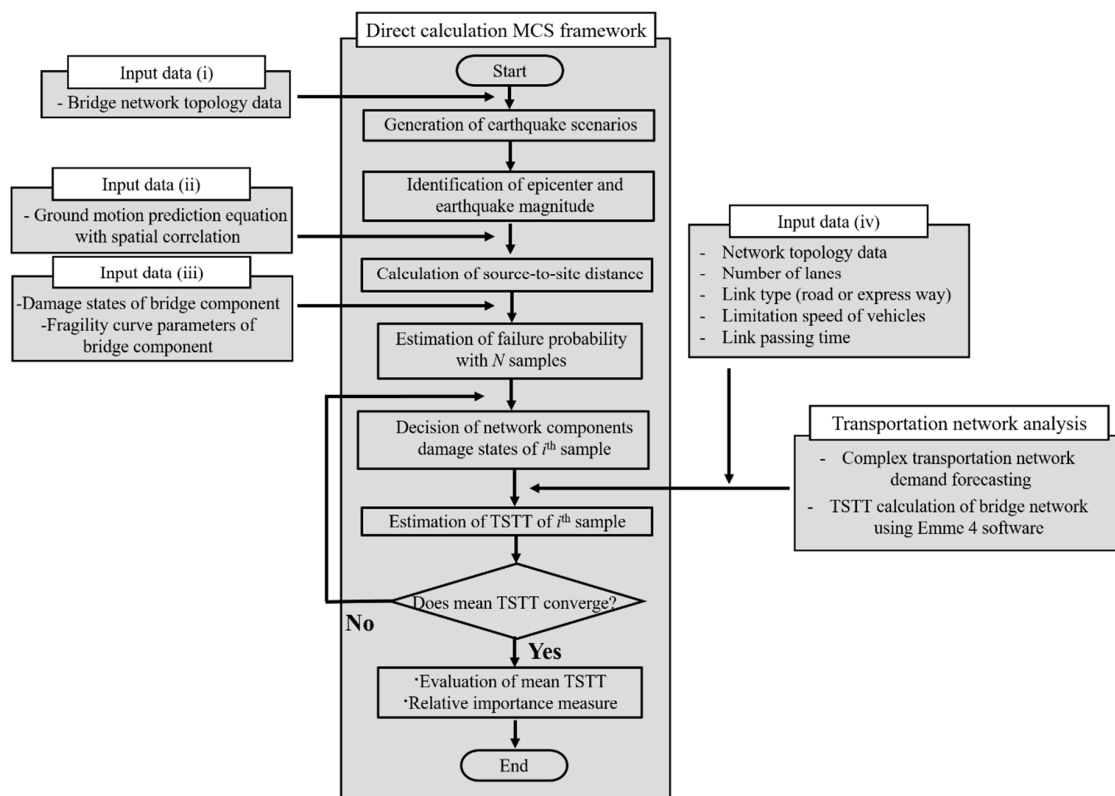


Figure 1. Conventional Monte Carlo simulation (MCS) framework for direct calculation.

Using the probabilities, a large number of samples of bridge damage states are generated. In each damage state sample, the performance and flow capacity of bridge structures are determined according to the damage states and can be utilized as input data for bridge transportation network analysis through the determined damage states. For this purpose, traffic analysis of a bridge transportation network requires basic information such as network topology data and number of lanes, link type (roadway or expressway), vehicle speed limit, and time required to pass each link for each bridge. If the damage states and flow capacity of each bridge facility are determined, the travel time of the source node to the destination node can be calculated through traffic analysis, and the summation of total travel time between all nodes is defined as TSTT. One of the widely used programs for traffic analysis is EMME/4 developed by the INRO company, Canada. It is a software package of travel demand modeling that enables the TSTT calculation of an entire network at the macro level. EMME/4 considers the specific roadway network with each bridge facility and the travel demand of traffic analysis zones based on traditional four-step travel demand modeling, which enables stable macro function analysis. When bridges are damaged due to an earthquake, the capacity of road links, in which the damaged

bridges are included, is reduced. Subsequently, the optimized outcomes of traffic assignments are changed in the form of increasing TSTT. By comparing the TSTT of each scenario, the seismic risk of bridge transportation networks can be assessed. It has been adopted to estimate the performance of a transportation network in several studies [15–17], and we also adopted the EMME/4 software to calculate TSTTs in this study. If the mean value of TSTT calculated in the i th sampling satisfies a convergence criterion, the average total travel time and relative importance measure for each scenario are calculated, and the entire algorithm ends. If not, an iterative process of calculating TSTT with the $(i + 1)$ th sample is required.

2.2. Artificial Neural Network (ANN) Model

ANN is known as an artificial intelligence technique that constructs a transfer function (with hidden layers and neurons) through pattern recognition of input and output data. This technique expresses the complex relationship between input and output data as a simple mathematical function with supervised learning. Because the recent deep- and machine-learning technologies are approaches developed based on existing neural networks, the ANN technique has many advantages that system users can exploit to easily handle these tools with relatively fast operation speed. For this reason, numerous researchers have used ANN techniques in a variety of engineering research fields such as structural health monitoring [29], structural control [30], damage detection [31–33], and structural response estimation [34–36].

To evaluate the performance of a bridge transportation network against various seismic conditions efficiently, this study adopts an ANN-based surrogate model. The surrogate model enables accelerated seismic risk assessment, especially when calculating network performance that requires a high computational cost such as TSTT in high-dimensional bridge transportation networks. Although some initial training time is required to build the surrogate model, once the model is constructed, no more sophisticated-traffic analysis is required. The surrogate model enables effective prediction of system performance even for high-dimensional bridge networks with novel performance indices, it can be used for various iterative analyses such as seismic risk assessment, network resilience estimation, PSHA, and optimization problems.

2.3. Proposed ANN-Based Surrogate Model

In this study, TSTT was introduced as the performance index of a bridge transportation network, and an ANN-based surrogate model with the MCS framework was proposed to predict TSTT. Figure 2 shows a flowchart for integrating a surrogate model with the MCS framework to evaluate the mean TSTT and relative importance measure. The input data required to execute system reliability are the topology data (nodes, links, adjacent matrix) of the bridge transportation network, spatially correlated seismic attenuation law of the target network, and damage states and fragility curve parameters of the bridge components.

The United States Federal Emergency Management Agency (FEMA) [37] proposed the failure probability of a bridge structure as five levels of damage states and estimated the fragility curve based on past empirical data as a lognormal curve (expressed as a median and a log standard deviation). A fragility curve is defined as the conditional probability based on the ground intensity measure [38], and FEMA determined that spectral acceleration (SA) predicts the failure probability of the bridge structure well. In the case of the seismic attenuation law, the ground motion prediction equation proposed by Emolo et al. [39] was utilized for non-linear regression analysis of 222 earthquake datasets from 132 stations in South Korea. The intensity of the mean ground motion from that study can be expressed by the following equation:

$$\ln(SA_{ij}) = c_1 + c_2 M_i + c_3 \ln\left(\sqrt{R_{ij}^2 + h^2}\right) + c_4 R_{ij} + c_5 s \quad (1)$$

where SA_{ij} represents the spectral acceleration at site j when an earthquake occurs at source i , M_i represents the earthquake magnitude at the epicenter i , R_{ij} is the epicentral distance between source i and site j , h is the length of focal depth (km), $c_1 \sim c_5$ represent non-linear regression coefficients (in this study, the regression coefficients are assumed to be $-5.15, 0.95, -0.92, 6.8, -0.0003$, and 0.208 , respectively [39]), and s denotes a dummy variable and is assumed to be either $-1, 0$, or 1 depending on the station.

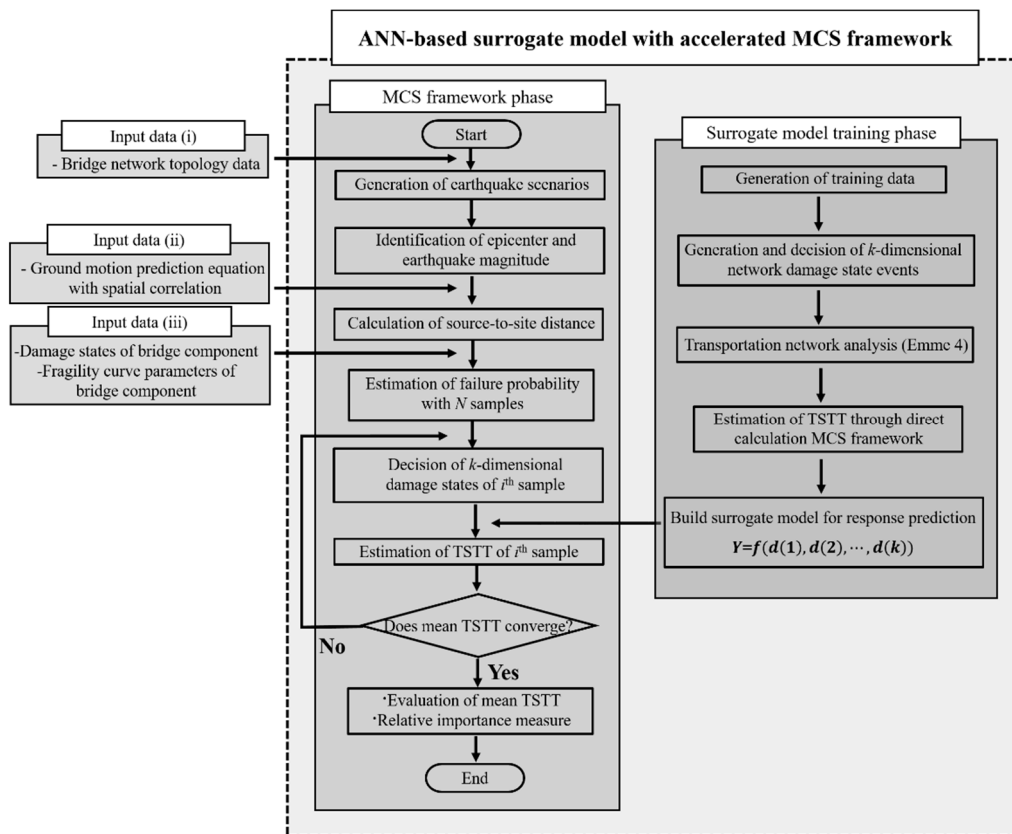


Figure 2. Flowchart for accelerated seismic risk assessment of bridge transportation networks.

In addition, in this study, inter- and intra-event terms were considered to represent the uncertainty of ground motion [40,41]. Inter-event terms indicate the uncertainty with which the energy transmitted to the ground surface varies owing to the characteristic of the earthquake itself, whereas intra-event terms indicate the uncertainty with which the transmitted energy to the ground surface varies depending on geotechnical environments and seismic attenuation paths. The uncertainty of ground motion intensity ρ_{total} can be expressed by the following equation [42,43]:

$$\rho_{total} = \frac{\sigma_{\eta}^2}{\sigma_{\eta}^2 + \sigma_{\epsilon}^2} + \frac{\sigma_{\epsilon}^2}{\sigma_{\eta}^2 + \sigma_{\epsilon}^2} \rho(\Delta_{ij}) \tag{2}$$

where σ_{η} and σ_{ϵ} represent predefined inter- and intra-event residuals with zero mean value, and $\rho(\Delta_{ij})$ represents the spatial correlation equation. In this study, the intra-event correlation equation proposed by Goda and Hong [44] was utilized, and the correlation function can be expressed by the following equation:

$$\rho(\Delta_{ij}) = e^{(-0.509 \sqrt{\Delta})} \tag{3}$$

where Δ_{ij} represents the distance between the i th site and the j th site.

Once the input data required to apply the ANN-based surrogate model with the MCS framework are acquired, the epicenter and magnitude of the earthquake are determined according to each scenario.

Depending on the epicenter and the earthquake magnitude, the failure probability of each bridge component can be evaluated according to the source-to-site distance. When the failure probability of each component of the entire system is determined, the k -dimensional damage states can be determined. Based on the damage states, TSTT can be evaluated through the surrogate model based on supervised learning. The surrogate model can be constructed using training data generated from determined epicenter and TSTT results. In this study, the k -dimensional bridge damage states and TSTT calculated by EMME/4 software (multimodal transport planning software) were generated as input and output data for training data. In addition, TSTT was defined using the following equation:

$$TSTT = \sum_{j=1}^{N_l} V_j T_j \quad (4)$$

where V_j represents the total volume (available number traffic per day) of the j th link, T_j represents the time required to pass the j th link, and N_l represents the number of links of the entire bridge transportation network.

Furthermore, the TSTT incremental factor (TIF) was proposed as a new performance measure in this method. TIF is defined as the increment of the average TSTT by the observed failure event of each bridge, which enables the relative importance of the bridge structures to be quantified. The proposed TIF can be expressed as

$$TIF_i = 1 - \frac{TSTT_{\mu_Q|C_i}}{TSTT_{\mu_Q}} \quad (5)$$

where TIF_i represents the relative importance measure of the i th bridge, $TSTT_{\mu_Q|C_i}$ represents the mean TSTT of the entire system when the i th bridge has a failure, and $TSTT_{\mu_Q}$ denotes the mean TSTT.

3. Application Example

3.1. Description of Target Bridge Transportation Network

To demonstrate the ANN-based surrogate model with an MCS framework proposed in Section 2.3, an actual bridge transportation network in Pohang, South Korea, was adopted in this study. The target network lies on a dense fault in southeast South Korea, and a magnitude 5.4 earthquake occurred in 2017 [45]. South Korea is known to have a relatively low earthquake probability, but recent frequent earthquakes and aftershocks have increased the level of interest in seismic risk assessment [46].

Figure 3 shows the topology of the target bridge transportation network, which comprises 1440 nodes and 3490 links. In addition, the bridge connecting each road network comprises 48 long-span bridges, including highways and national highways. The aim of this numerical analysis is to find TSTT of all nodes according to the damage states of 48 bridge structures. Figure 4 shows detailed structural information such as the superstructure type and traffic volume distribution for 48 bridges that compose the transportation network. The superstructure of the bridge is classified into six types, and the maximum volume of vehicles that can pass is up to 43,000 per day. In addition, travel demand of traffic analysis zones is determined based on the population and the number of households from the 2015 Census conducted by the Korean government [47]. The mean total span length of 48 bridges is 101.15 m with a minimum of 10 m and a maximum of 455 m, the mean length of each span is 23.68 m with a minimum of 9 m and a maximum of 70 m, and the mean pier height is 5.73 m with a minimum of 2.5 m and a maximum of 25 m.

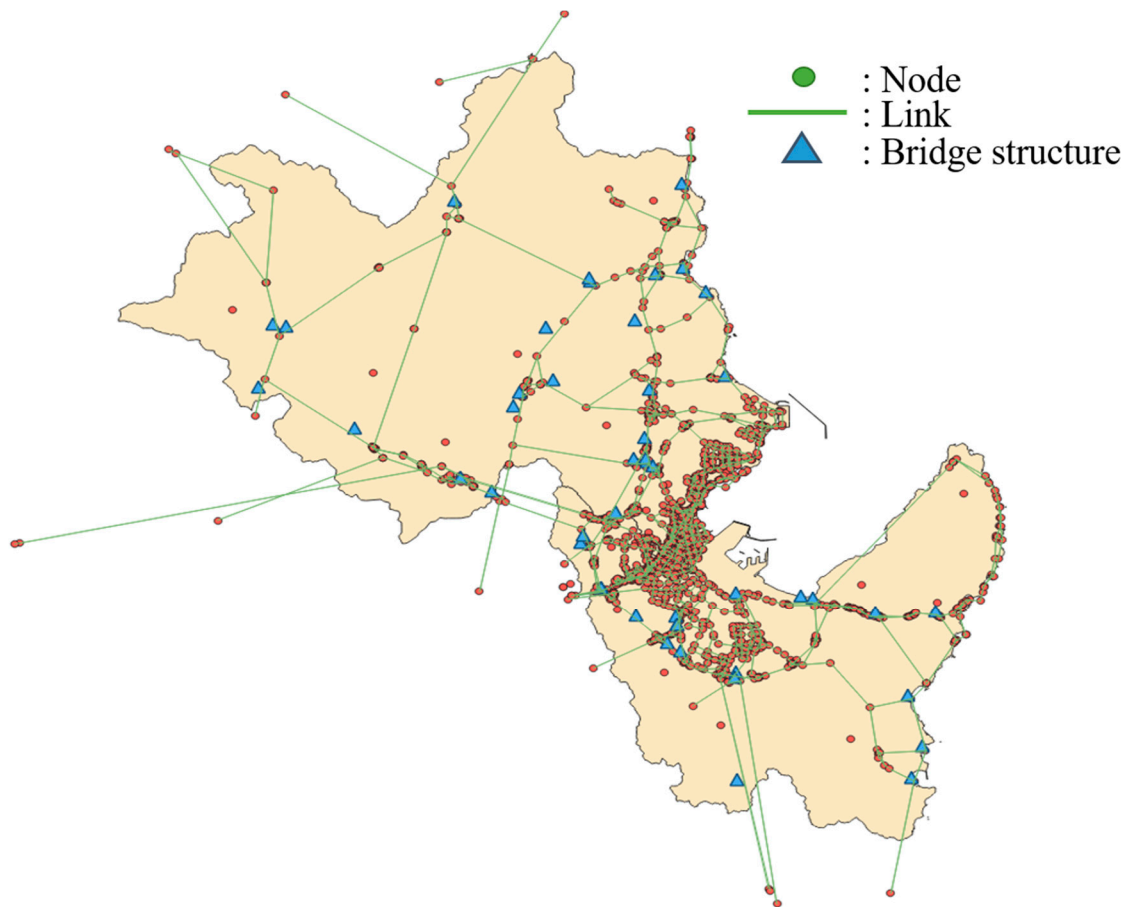


Figure 3. Reconstructed target bridge transportation network.

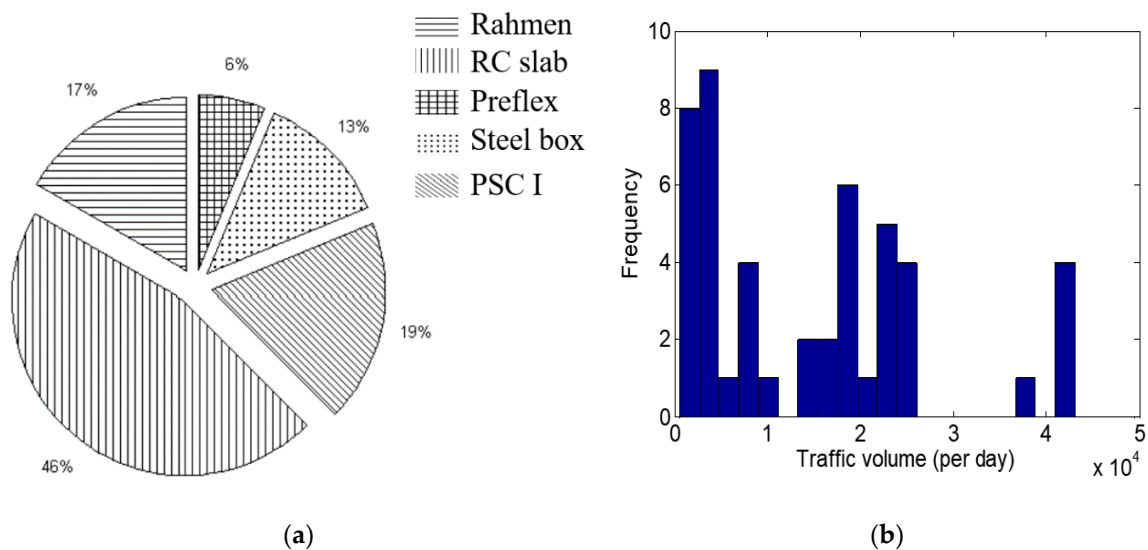


Figure 4. Structural information of 48 bridge structures. (a) Superstructure type, (b) traffic volume distribution.

3.2. Uncertain Magnitude and Location of Epicenter for Probabilistic Seismic Hazard Analysis (PSHA)

Figure 5 shows the considered locations of the 20 major historical epicenters and bridge structures for PSHA analysis. To identify the uncertainty of the magnitude of the earthquake in the target area, historical data of earthquakes with magnitude 3.0 or higher from 1 January 1918 to 22 August 2018, were collected by the Korea Meteorological Association (KMA), and it was assumed that location uncertainty of the 20 epicenters was the same. Based on the 20 epicenters proposed by Tak et al. [13],

the uncertainty of the magnitude of the earthquake in the target network was presented by the bounded Gutenberg–Richter (G–R) recurrence law [48,49]. The results of PSHA in the target area show that the coefficient values of a and b (in the G–R recurrence law) calculated by regression analysis are 2.167 and 0.699, respectively. In this study, the magnitude of the earthquake in the target network was considered as 4.5 to 7.5, and the bounded probability density function of the earthquake magnitude between the normalized magnitudes of 4.5 and 7.5 through the G–R relation law can be expressed as shown in Figure 6 [13].

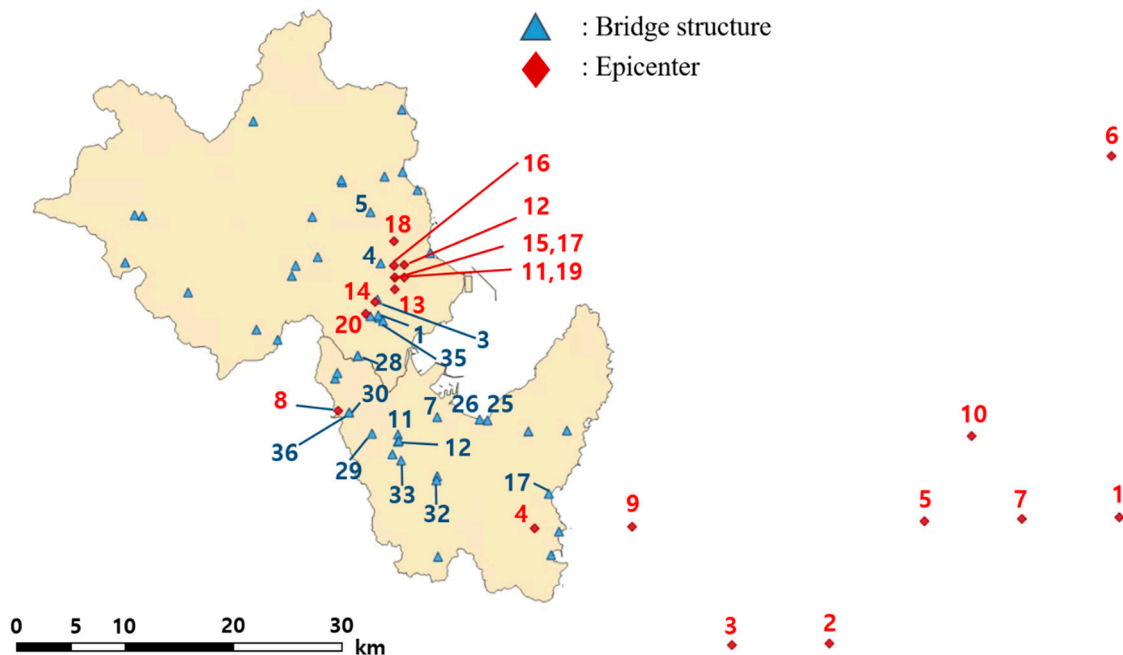


Figure 5. Locations of the considered bridge structures and epicenters in the target network.

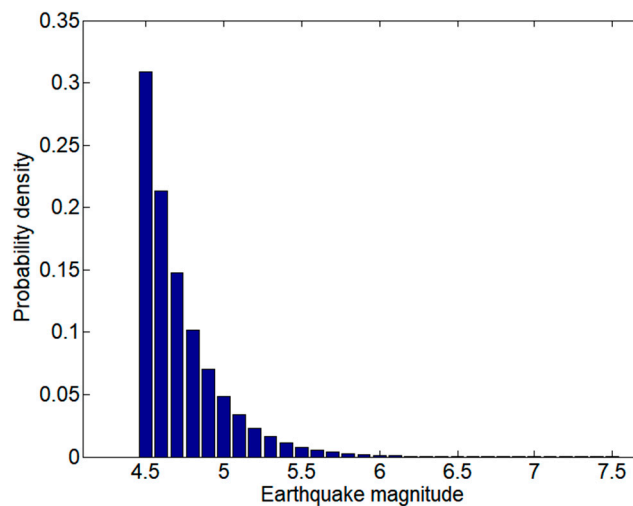


Figure 6. Discrete bounded probability density function of earthquake magnitude ranging from 4.5 to 7.5.

3.3. Construction of ANN-Based Surrogate Model

In this section, an ANN-based surrogate model was constructed to predict the TSTT performance of the bridge transport network. Five damage states of 48 bridges were considered as the input values of the ANN model for constructing the surrogate model and were assumed to be integer values from 0 to 4 depending on each damage state. In addition, for the input data generation for training, Epicenter 8 shown in Figure 5 was selected as the training epicenter, and the input earthquake magnitude was

considered as 7.0 with a focal depth of 10 km. Moreover, the ground motion intensity SA of each bridge was utilized to determine the damage state of each bridge according to the spatially correlated seismic attenuation law from the input earthquake. Finally, TSTT values for each scenario were calculated by EMME/4 and considered as output data. In addition, to reflect the traffic flow capacity of the damaged bridge, the reduced traffic volume was considered according to each damage state. Table 1 shows the reduced capacities of a damaged bridge structure according to damage states for transportation network analysis.

Table 1. Reduced capacities of damaged bridge structure.

Damage State	Reduced Capacity
Complete damage	0%
Extensive damage	25%
Moderate damage	50%
Slight damage	75%
No damage	100%

In this study, an ANN-based surrogate model was trained with a total of 100,000 randomly sampled data. In addition, 30,000 sufficient epochs were adopted, and 100,000 data were set with the ratio 0.7:0.15:0.15 (training: validation: test) to prevent under- and overfitting problems of training, validation, and test data in surrogate models. The surrogate model was validated through the correlation coefficient of each dataset. Table 2 shows the configuration of the neural network for constructing the surrogate model. In addition, the sigma and lambda values of the training function were utilized as 5×10^{-5} and 5×10^{-7} , respectively, and the minimum gradient was set to 1×10^{-8} for learning parameters. The number of hidden layers and neurons was determined through trial and error, and learning parameters that could be converged by a 48-dimensional function with five variables were considered as representative values.

Table 2. Neural network construction for surrogate model.

Network Properties	Utilized Function or Value
Network input dimensions (output dimensions)	48(1)
Network type	Feed-forward backpropagation
Training function	Scaled conjugate gradient backpropagation
Adaption learning function	Gradient descent with momentum weight and bias learning function
Performance function	Mean squared error
Number of layers	20
Number of neurons	20
Transfer function	Hyperbolic tangent sigmoid transfer function

Figure 7 shows that the mean squared error (MSE) values of the training, validation, and test sets of the ANN-based surrogate model converge as the epoch increases. In this study, 30,000 epochs were considered to avoid underfitting and overfitting problems. Figure 8 shows the correlation coefficient (R) values for the training, validation, and test data of the neural network as 0.9853, 0.9759, and 0.9760, respectively, and the correlation coefficient for 100,000 data was calculated as 0.9825. As a result of the coefficient correlation of the constructed surrogate model, it was confirmed that the accuracy of the network performance response can be predicted with high accuracy.

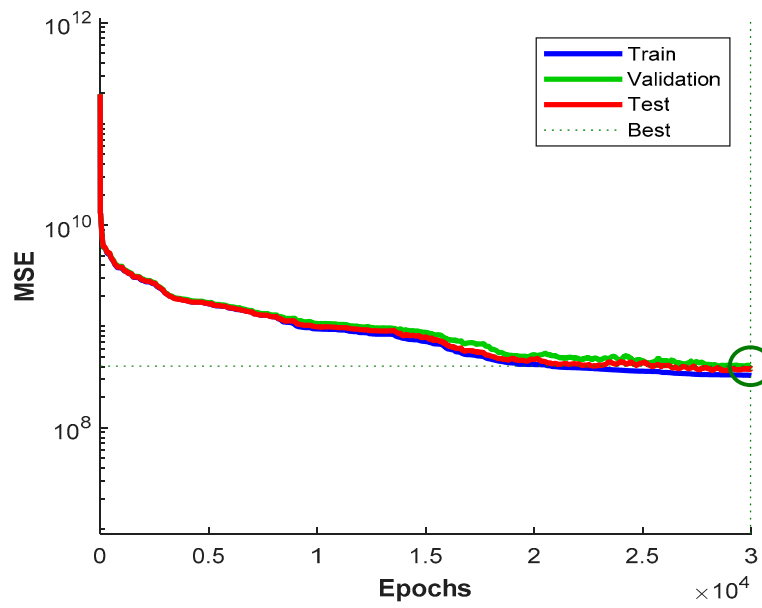


Figure 7. Performance of surrogate model according to epochs.

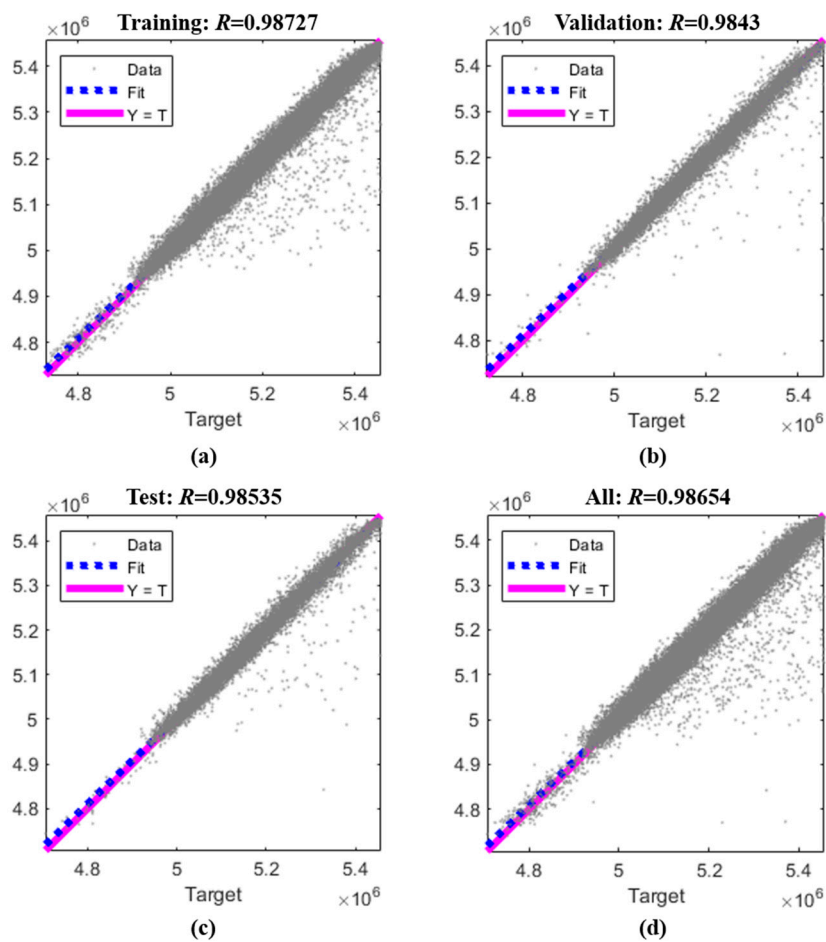


Figure 8. Correlation coefficients of (a) training, (b) validation, (c) test, and (d) all data set.

3.4. Analysis Results

In this section, the mean traffic quantity of various epicenters and earthquake magnitudes were estimated using the surrogate model which was described in Section 3.3. Twenty locations of the input earthquake ground motion were considered (Figure 5), and the earthquake magnitude range at the epicenter was considered to be M 4.5 to 7.5. The accuracy of the surrogate model was verified through the correlation coefficient of the generated surrogate model, and a surrogate model was applied to evaluate network performance according to the various earthquake magnitudes. In addition, to identify convergence of network performance, the relative error of the coefficient of variation (COV) of network performance according to the number of samples was confirmed. As an example, Figure 9 shows the convergence of the mean TSTT according to the number of samples at Epicenter 8 with an earthquake of magnitude 7.5.

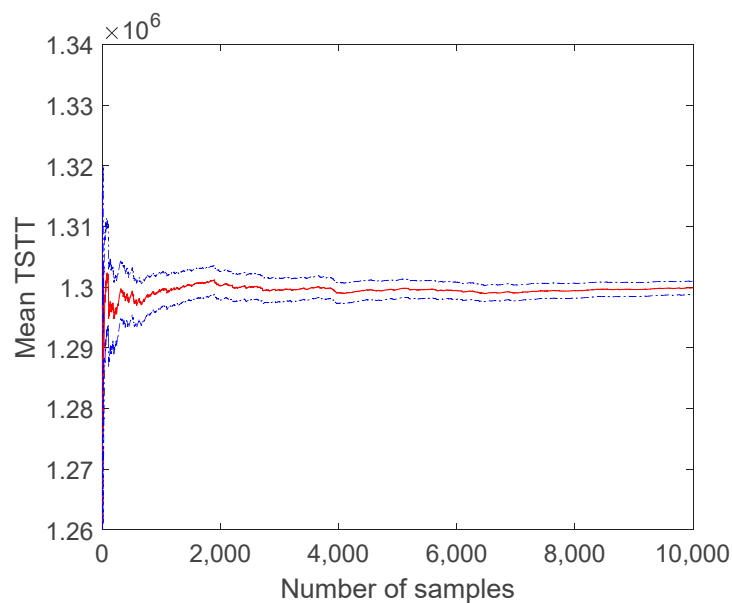


Figure 9. Convergence of mean total system travel time (TSTT) according to the number of samples.

It is also noted in Figure 9 that 10,000 samples were required for only one set of epicenter and earthquake magnitude, and it took approximately 2 s to calculate a TSTT for each sample using EMME/4 and a general-purpose personal computer. For seismic risk assessment, similar analysis should be conducted repeatedly for many different sets of epicenters and earthquake magnitudes. In this example, the range of earthquake magnitudes (i.e., M 4.5 to 7.5) is divided by 0.1 intervals and 20 epicenters are considered, which means that the same MCS analysis with 10,000 samples should be conducted 620 times. For the proposed method, however, only one set of 100,000 samples was required to construct the surrogate model. Once the surrogate model is constructed, it took less than a minute to calculate TSTTs for each epicenter and earthquake magnitude with 10,000 samples.

Figure 10 shows the mean TSTT values for earthquakes of 4.5 to 7.5 magnitude at 20 epicenters and uncertain locations. The mean TSTT of the bridge transportation network tended to increase as the magnitude of the earthquake increased, and the mean TSTT tended to decrease as the epicentral distance from the principal network component increased. This is because the reduction in capacity of each bridge component depends on the intensity and distance of the earthquake. Figure 10a,b show that the mean TSTT decreased because the epicenter was farther from the target network compared with the mean TSTT of uncertain locations (except for EQ8). In addition, earthquake magnitudes below 6.5 did not significantly affect the average TSTT because the location of the epicenter was far. However, as the earthquake magnitude gradually increased, the mean TSTT tended to increase rapidly. On the other hand, in Figure 10c,d, the mean TSTT at locations 11–20 was significantly increased compared

to the mean TSTT of the uncertain location because the considered epicenter was located around the target network. Moreover, since the location of the epicenter was adjacent to the principal bridge structure, the mean TSTT tended to increase rapidly even at relatively small earthquakes of M 6.0.

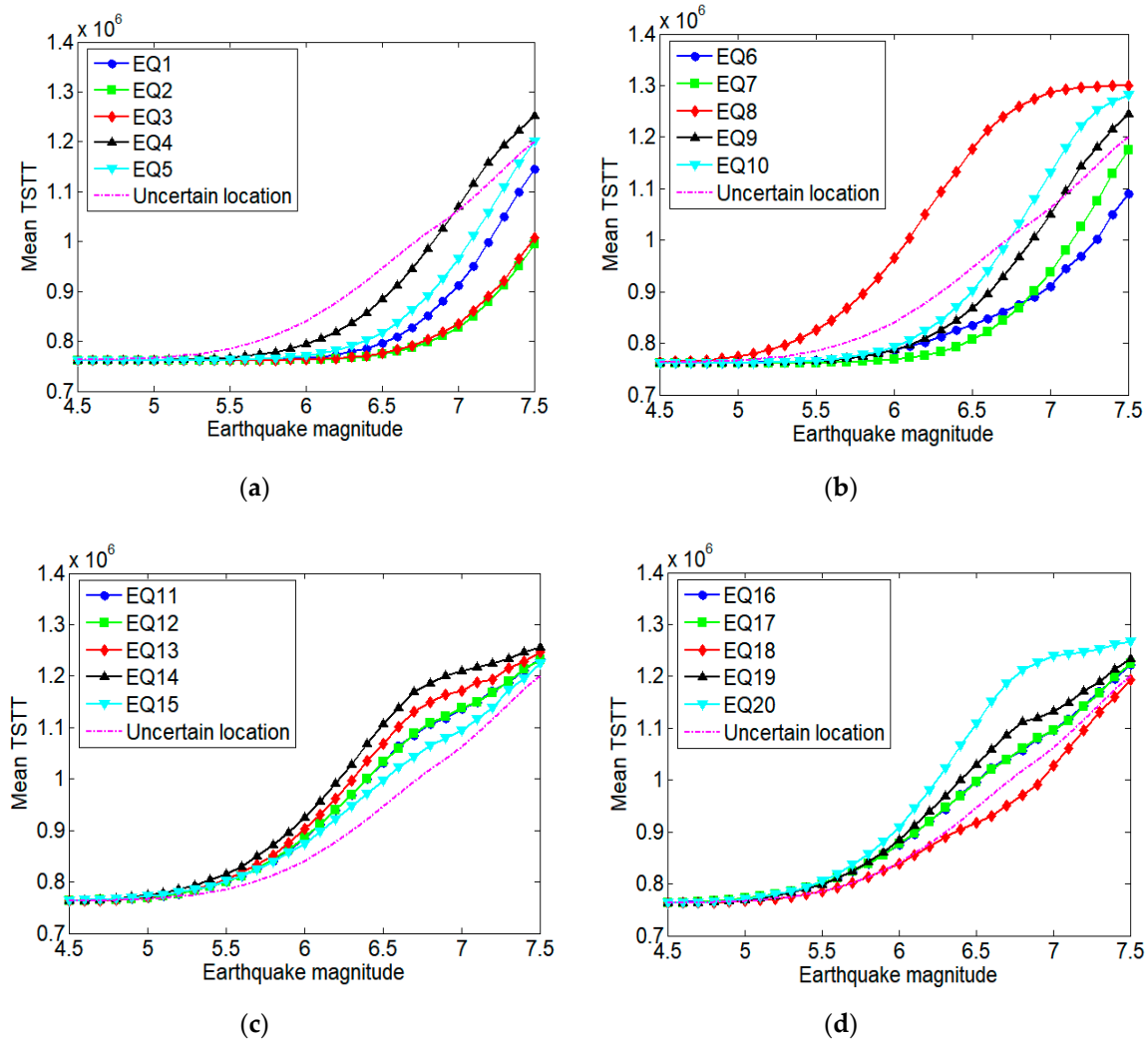


Figure 10. Evaluation of mean TSTT with different epicenters and earthquake magnitude. (a) Locations 1 to 5, (b) locations 6 to 10, (c) locations 11 to 15, and (d) locations 16 to 20.

Figure 11 shows the distribution of the mean TSTT for uncertain earthquake magnitudes over 20 epicenters, and the red curve shows the mean TSTT for uncertain locations. As seen in Figure 10, it was found that the closer the epicenter location to the target network, the greater the impact of the mean TSTT. On the other hand, it was confirmed that the epicenter located relatively far away had a small effect on the mean TSTT. In particular, it was confirmed that the locations of epicenters 8 and 14 had a significant effect on the entire traffic flow of the target network.

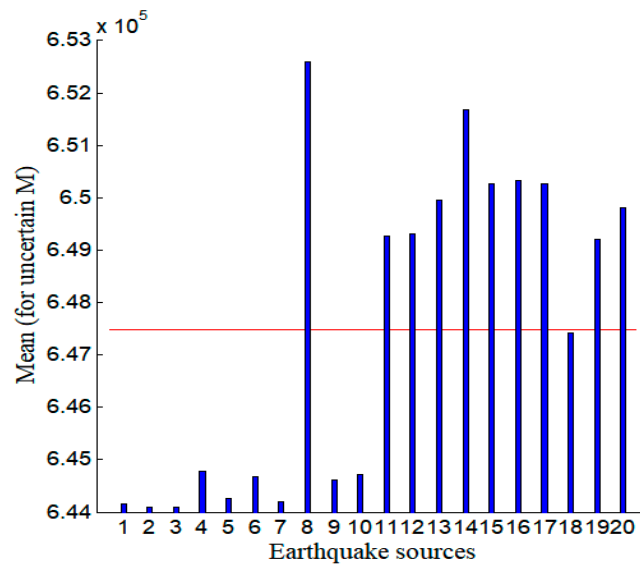


Figure 11. Distribution of mean TSTT according to earthquake sources for uncertain earthquake magnitudes.

Figure 12 shows the relative importance measures (TIF) of 48 bridges according to the relatively high mean TSTT of epicenters 8 and 14 and uncertain scale and location. If the bridge structure had a failure in a relatively high-importance component, disconnection occurred between major nodes (high centrality) with many passages. As a result, travel time increased rapidly because vehicles could not reach most nodes of the entire bridge transportation network. On the other hand, it can be seen that relatively low-importance bridges did not have a significant impact on the mean TSTT even if the bridge was destroyed because bridges with low relative importance were mostly in suburban regions of the city or far from the principal connecting node (low centrality). Figure 12 shows the TIF for relatively high-importance bridges, and when compared to Figure 11, the analysis results showed that the bridges with relatively high relative importance were at the center of the target network, especially in the region with easy access to dense nodes in the center of the city. On the other hand, the remaining bridges were outside the target network or around isolated nodes.

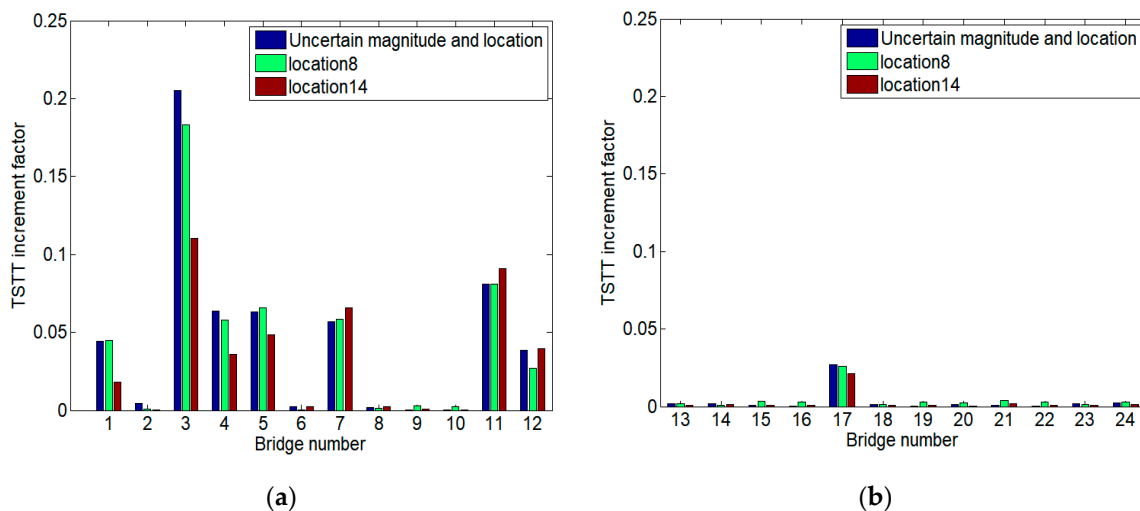


Figure 12. Cont.

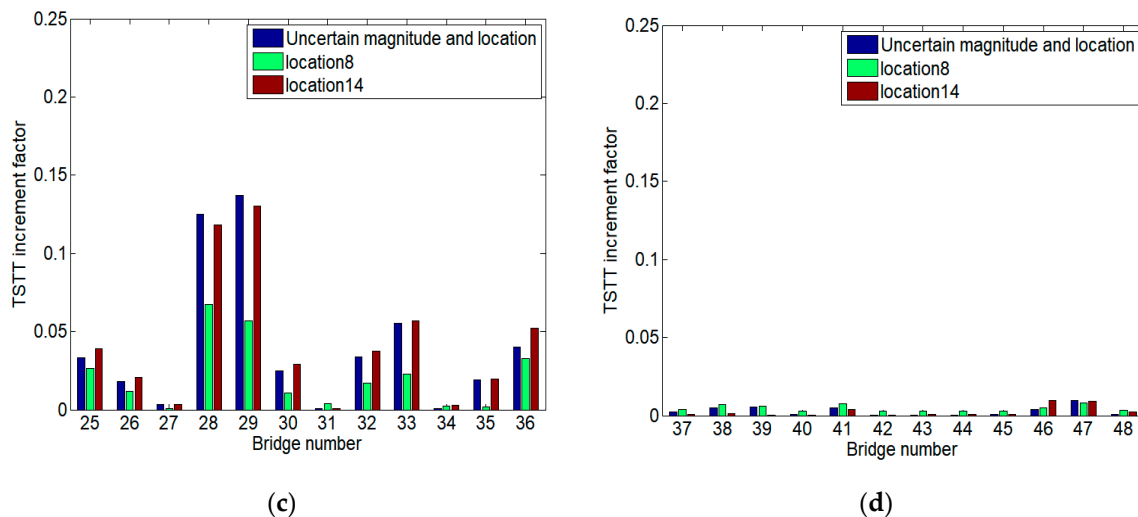


Figure 12. Relative importance of bridge number (a) 1 to 12, (b) 13 to 24, (c) 25 to 36, and (d) 37 to 48.

4. Conclusions

In this study, an ANN-based surrogate model was proposed for accelerated seismic risk assessment of a system-level bridge transportation network. To accurately evaluate the performance of the bridge network, TSTT through traffic analysis was considered as a performance index, and the MCS framework phase was adopted for performance evaluation according to each event. TSTT has high accuracy but high calculation cost, so it is difficult to adopt it easily as a performance index. However, this study proposed a methodology to predict TSTT without direct TSTT calculation by introducing an ANN-based surrogate model to reduce excessive time cost. In addition, a maximum failure event generation strategy that can efficiently reduce the number of system events was introduced to efficiently handle the entire event vector.

To demonstrate the proposed methodology, an actual bridge transportation network was reconstructed with 48 bridge structures and five damage states (1440 nodes and 3490 links). For various earthquake scenarios, the performance of the entire network system was estimated stochastically with respect to the amount of total travel time. Training data were generated with an earthquake magnitude of 7.0, and TSTT values of various earthquake magnitudes at the various epicenter locations were evaluated to verify the robustness of the epicenter and earthquake magnitude. As a result of the numerical analysis, it was confirmed that the ANN-based surrogate model predicts TSTT very accurately for the earthquake magnitude and the location of the epicenter.

Seismic risk assessments have been performed using the proposed methodology. However, the methodology proposed in this study is expected to be applied for seismic resilience and optimal decision making for civil infrastructure networks requiring numerous iterative analyses. Therefore, it will be possible to evaluate the performance of the network system efficiently prior to earthquakes and plan maintenance strategies immediately after earthquakes even in a high-dimensional bridge transportation network.

Author Contributions: Conceptualization, H.-Y.T. and Y.-J.L.; formal analysis, S.Y.; software, S.Y. and M.K.; methodology, S.Y., J.K., and Y.-J.L.; supervision, Y.-J.L.; validation, S.Y., J.K., and Y.-J.L.; writing—Original draft, S.Y.; writing—Review and editing, W.S., M.K., J.K., H.-Y.T., and Y.-J.L. All authors have read and agreed to the published version of the manuscript.

Funding: This research was supported by a grant (20SCIP-B146946-03) from the Construction Technology Research Program funded by the Ministry of Land, Infrastructure and Transport of Korean government.

Acknowledgments: This research was supported by a grant (20SCIP-B146959-03) from Construction technology research program funded by Ministry of Land, Infrastructure and Transport of Korean government.

Conflicts of Interest: The authors declare no conflict of interest.

References

1. Kim, J.; Deshmukh, A.; Hastak, M. A framework for assessing the resilience of a disaster debris management system. *Int. J. Disaster Risk Reduct.* **2018**, *28*, 674–687. [[CrossRef](#)]
2. Yoon, S.; Lee, Y.-J.; Jung, H.-J. A comprehensive framework for seismic risk assessment of urban water transmission networks. *Int. J. Disaster Risk Reduct.* **2018**, *31*, 983–994. [[CrossRef](#)]
3. Esposito, S.; Iervolino, I.; d’Onofrio, A.; Santo, A.; Cavalieri, F.; Franchin, P. Simulation-based seismic risk assessment of gas distribution networks. *Comput. Aided Civ. Infrastruct. Eng.* **2015**, *30*, 508–523. [[CrossRef](#)]
4. Nuti, C.; Rasulo, A.; Vanzi, I. Seismic safety evaluation of electric power supply at urban level. *Earthq. Eng. Struct. Dyn.* **2007**, *36*, 245–263. [[CrossRef](#)]
5. Dueñas-Osorio, L.; Craig, J.I.; Goodno, B.J. Seismic response of critical interdependent networks. *Earthq. Eng. Struct. Dyn.* **2007**, *36*, 285–306. [[CrossRef](#)]
6. Rokneddin, K.; Ghosh, J.; Dueñas-Osorio, L.; Padgett, J.E. Bridge retrofit prioritisation for ageing transportation networks subject to seismic hazards. *Struct. Infrastruct. Eng.* **2013**, *9*, 1050–1066. [[CrossRef](#)]
7. Kang, W.-H.; Song, J.; Gardoni, P. Matrix-based system reliability method and applications to bridge networks. *Reliab. Eng. Syst. Saf.* **2008**, *93*, 1584–1593. [[CrossRef](#)]
8. Yoon, S.; Lee, Y.-J.; Jung, H.-J. A comprehensive approach to flow-based seismic risk analysis of water transmission network. *Struct. Eng. Mech.* **2020**, *73*, 339–351.
9. Shi, P.; O’Rourke, T.D. *Seismic Response Modeling of Water Supply Systems*; Multidisciplinary Center for Earthquake Engineering Research: Buffalo, NY, USA, 2008.
10. Wang, Y.; O’Rourke, T.D. *Seismic Performance Evaluation of Water Supply Systems*; Multidisciplinary Center for Earthquake Engineering Research: Buffalo, NY, USA, 2008.
11. Nuti, C.; Rasulo, A.; Vanzi, I. Seismic safety of network structures and infrastructures. *Struct. Infrastruct. Eng.* **2010**, *6*, 95–110. [[CrossRef](#)]
12. Choi, E.; Song, J. Development of Multi-Group Non-dominated Sorting Genetic Algorithm for identifying critical post-disaster scenarios of lifeline networks. *Int. J. Disaster Risk Reduct.* **2019**, *41*, 101299. [[CrossRef](#)]
13. Tak, H.-Y.; Suh, W.; Lee, Y.-J. System-Level Seismic Risk Assessment of Bridge Transportation Networks Employing Probabilistic Seismic Hazard Analysis. *Math. Probl. Eng.* **2019**, *2019*, 6503616. [[CrossRef](#)]
14. Lee, Y.-J.; Song, J.; Gardoni, P.; Lim, H.-W. Post-hazard flow capacity of bridge transportation network considering structural deterioration of bridges. *Struct. Infrastruct. Eng.* **2011**, *7*, 509–521. [[CrossRef](#)]
15. Sharma, S.; Mathew, T.V. Multiobjective network design for emission and travel-time trade-off for a sustainable large urban transportation network. *Environ. Plan. B Plan. Des.* **2011**, *38*, 520–538. [[CrossRef](#)]
16. Chang, L. *Transportation System Modeling and Applications in Earthquake Engineering*; Mid-America Earthquake (MAE) Center: Urbana, IL, USA, 2010.
17. Kim, Y.-S.; Spencer, B.F., Jr.; Elnashai, A.S. *Seismic Loss Assessment and Mitigation for Critical Urban Infrastructure Systems*; Newmark Structural Engineering Laboratory, University of Illinois at Urbana: Urbana, IL, USA, 2008; ISSN 1940-9826.
18. Yoon, S.; Lee, Y.-J.; Jung, H.-J. Flow-Based Optimal System Design of Urban Water Transmission Network under Seismic Conditions. *Water Resour. Manag.* **2020**, *34*, 1971–1990. [[CrossRef](#)]
19. Stern, R.E.; Song, J.; Work, D.B. Accelerated Monte Carlo system reliability analysis through machine-learning-based surrogate models of network connectivity. *Reliab. Eng. Syst. Saf.* **2017**, *164*, 1–9. [[CrossRef](#)]
20. Dueñas-Osorio, L.; Rojo, J. Reliability assessment of lifeline systems with radial topology. *Comput. Aided Civ. Infrastruct. Eng.* **2011**, *26*, 111–128. [[CrossRef](#)]
21. Kang, W.-H.; Lee, Y.-J.; Zhang, C. Computer-aided analysis of flow in water pipe networks after a seismic event. *Math. Probl. Eng.* **2017**, *2017*, 2017046. [[CrossRef](#)]
22. Song, J.; Kang, W.-H. System reliability and sensitivity under statistical dependence by matrix-based system reliability method. *Struct. Saf.* **2009**, *31*, 148–156. [[CrossRef](#)]
23. Li, J.; He, J. A recursive decomposition algorithm for network seismic reliability evaluation. *Earthq. Eng. Struct. Dyn.* **2002**, *31*, 1525–1539. [[CrossRef](#)]
24. Li, J.; Qian, Y.; Liu, W. Minimal cut-based recursive decomposition algorithm for seismic reliability evaluation of lifeline networks. *Earthq. Eng. Eng. Vib.* **2007**, *6*, 21. [[CrossRef](#)]

25. Lim, H.W.; Song, J. Efficient risk assessment of lifeline networks under spatially correlated ground motions using selective recursive decomposition algorithm. *Earthq. Eng. Struct. Dyn.* **2012**, *41*, 1861–1882. [[CrossRef](#)]
26. Liu, W.; Li, J. An improved recursive decomposition algorithm for reliability evaluation of lifeline networks. *Earthq. Eng. Eng. Vib.* **2009**, *8*, 409–419. [[CrossRef](#)]
27. Der Kiureghian, A.; Song, J. Multi-scale reliability analysis and updating of complex systems by use of linear programming. *Reliab. Eng. Syst. Saf.* **2008**, *93*, 288–297. [[CrossRef](#)]
28. Song, J.; Ok, S.Y. Multi-scale system reliability analysis of lifeline networks under earthquake hazards. *Earthq. Eng. Struct. Dyn.* **2010**, *39*, 259–279. [[CrossRef](#)]
29. Rizzo, P.; Lanza di Scalea, F. Wavelet-based feature extraction for automatic defect classification in strands by ultrasonic structural monitoring. *Smart Struct. Syst.* **2006**, *2*, 253–274. [[CrossRef](#)]
30. Akin, O.; Sahin, M. Active neuro-adaptive vibration suppression of a smart beam. *Smart Struct. Syst.* **2017**, *20*, 657–668.
31. Kim, J.-T.; Park, J.-H.; Koo, K.-Y.; Lee, J.-J. Acceleration-based neural networks algorithm for damage detection in structures. *Smart Struct. Syst.* **2008**, *4*, 583–603. [[CrossRef](#)]
32. Peng-hui, L.; Hong-ping, Z.; Hui, L.; Shun, W. Structural damage identification based on genetically trained ANNs in beams. *Smart Struct. Syst.* **2015**, *15*, 227–244.
33. Nguyen, D.H.; Bui, T.T.; De Roeck, G.; Wahab, M.A. Damage detection in Ca-Non Bridge using transmissibility and artificial neural networks. *Struct. Eng. Mech.* **2019**, *71*, 175–183.
34. Hakim, S.; Razak, H.A. Modal parameters based structural damage detection using artificial neural networks-a review. *Smart Struct. Syst.* **2014**, *14*, 159–189. [[CrossRef](#)]
35. Onat, O.; Gul, M. Application of artificial neural networks to the prediction of out-of-plane response of infill walls subjected to shake table. *Smart Struct. Syst.* **2018**, *21*, 521–535.
36. Shahbazi, Y.; Delavari, E.; Chenaghlou, M.R. Predicting the buckling load of smart multilayer columns using soft computing tools. *Smart Struct. Syst.* **2014**, *13*, 81–98. [[CrossRef](#)]
37. FEMA. *Multi-Hazard Loss Estimation Methodology Earthquake Model, HAZUS-MH MR3 Technical Manual*; Department of Homeland Security, Federal Emergency Management Agency: Washington, DC, USA, 2003.
38. Moon, D.-S.; Lee, Y.-J.; Lee, S. Fragility analysis of space reinforced concrete frame structures with structural irregularity in plan. *J. Struct. Eng.* **2018**, *144*, 04018096. [[CrossRef](#)]
39. Emolo, A.; Sharma, N.; Festa, G.; Zollo, A.; Convertito, V.; Park, J.H.; Chi, H.C.; Lim, I.S. Ground-motion prediction equations for South Korea Peninsula. *Bull. Seismol. Soc. Am.* **2015**, *105*, 2625–2640. [[CrossRef](#)]
40. Boore, D.M.; Gibbs, J.F.; Joyner, W.B.; Tinsley, J.C.; Ponti, D.J. Estimated ground motion from the 1994 Northridge, California, earthquake at the site of the Interstate 10 and La Cienega Boulevard bridge collapse, West Los Angeles, California. *Bull. Seismol. Soc. Am.* **2003**, *93*, 2737–2751. [[CrossRef](#)]
41. Wagener, T.; Goda, K.; Erdik, M.; Daniell, J.; Wenzel, F. A spatial correlation model of peak ground acceleration and response spectra based on data of the Istanbul earthquake rapid response and early warning system. *Soil Dyn. Earthq. Eng.* **2016**, *85*, 166–178. [[CrossRef](#)]
42. Sokolov, V.; Wenzel, F.; Kuo-Liang, W. Uncertainty and spatial correlation of earthquake ground motion in Taiwan. *TAO Terr. Atmos. Ocean. Sci.* **2010**, *21*, 9. [[CrossRef](#)]
43. Cimellaro, G.P.; De Stefano, A.; Reinhorn, A.M. Intra-event spatial correlation of ground motion using L'Aquila earthquake ground motion data. In Proceedings of the 3rd ECCOMAS Thematic Conference on Computational Methods in Structural Dynamics and Earthquake Engineering, Corfu, Greece, 25–28 May 2011; pp. 3091–3108.
44. Goda, K.; Hong, H.-P. Spatial correlation of peak ground motions and response spectra. *Bull. Seismol. Soc. Am.* **2008**, *98*, 354–365. [[CrossRef](#)]
45. Kang, S.; Kim, B.; Bae, S.; Lee, H.; Kim, M. Earthquake-induced ground deformations in the low-seismicity region: A case of the 2017 M5. 4 Pohang, South Korea, earthquake. *Earthq. Spectra* **2019**, *35*, 1235–1260. [[CrossRef](#)]
46. Lee, S.; Kim, B.; Lee, Y.-J. Seismic fragility analysis of steel liquid storage tanks using earthquake ground motions recorded in Korea. *Math. Probl. Eng.* **2019**, *2019*, 6190159. [[CrossRef](#)]
47. Statistic Korea. *Results of the 2015 Population and Housing Census (Internal Migration, Commuting and Activity Constraint)*; Statics Korea: Daejeon, Korea, 2017.

48. Gutenberg, B.; Richter, C.F. Frequency of earthquakes in California. *Bull. Seismol. Soc. Am.* **1944**, *34*, 185–188.
49. Baker, J.W. An introduction to probabilistic seismic hazard analysis (PSHA). *White Pap. Version* **2008**, *1*, 72.



© 2020 by the authors. Licensee MDPI, Basel, Switzerland. This article is an open access article distributed under the terms and conditions of the Creative Commons Attribution (CC BY) license (<http://creativecommons.org/licenses/by/4.0/>).